Available online at www.sciencedirect.com
SCIENCE DIRECT®
Geodinamica Acta 16 (2003) 119–129
Geodinamica Acta
www.elsevier.com/locate/geoact

Strain partitioning in transpressive shears zones in the southern branch of the Variscan Ibero-Armorican arc

R. Dias [a,*], A. Mateus [b], A. Ribeiro [c]

[a] Dep. Geociências, LIRIO and Centro de Geofísica, Univ. Évora, Convento das Maltezas, 7100-513 Estremoz, Portugal
[b] Dep. Geologia and CREMINER, Univ. Lisboa, Edifício C2, Piso 5, Campo Grande, 1700 Lisbon, Portugal
[c] Dep. Geologia and LATTEX, Univ. Lisboa, Edifício C2, Piso 5, Campo Grande, 1700 Lisbon, Portugal

Received 7 June 2002; accepted 10 April 2003

Abstract

The Torre de Moncorvo region (NE Portugal) is a key-sector of the Autochthon Domain of the Iberian Terrane. The region experienced Variscan deformation in the southern branch of the Ibero-Armorican Arc wherein the early structures (of Upper Devonian age—D_1) denotes the establishment of a heterogeneous sinistral transpressive regime. This regime was also responsible for the development of large-scale left-lateral shear zones whose direction is subparallel to major folds. Finite strains analyses were carried out in the Torre de Moncorvo region using the normalised Fry method on different strain markers: (1) distribution of detrital quartz grains in quartzite rocks of Arenigian–Lanvirnian age; (2) arrangement of oolites in discontinuous Ordovician–Silurian ironstone horizons; (3) the rotation experienced by *Skolithos* preserved in Lower Ordovician metasedimentary clastic rocks. The results obtained indicate the predominance of slightly prolate strain ellipsoids. Nevertheless, the variation of their orientation around mesoscopic folds emphasises the role of strain partitioning in a transpressive regime, suggesting that different folding mechanisms were active in the course of the same deformation phase. For the studied cases, tangential longitudinal strain and flexural shear combined with regional sinistral shear seem to be the most common mechanisms of folding. Some of these three-dimensional theoretical models for strain patterns in folds could be used in other regions, where a transpressive regime is inferred.
Published by Éditions scientifiques et médicales Elsevier SAS.

Keywords: Transpression; Variscan; Folding mechanisms; Strain analysis

1. Introduction

Since the pioneering work of Harland [17], transpression has been recognised as a widespread deformation regime in fold belts. From homogeneous transpression [40], field data soon led to more elaborate theoretical models where the strain partitioning proved to be a common situation (e.g. [5,21,42,44]). Although these models allow for a good prediction of the bulk strain related with these regimes, little work has been produced in order to understand the highly heterogeneous strain that should be induced by the folding in such regimes [20,46].

In northern Portugal the main autochthonous Variscan structures have been produced by a heterogeneous transpressive regime [9,10,37]. Comprehensive geometrical and kinematical analyses of these structures were performed in Ordovician and Silurian metasediments in two sectors near Torre de Moncorvo. These studies were combined with finite strain estimations, since the knowledge of the strain pattern is fundamental to the understanding of any deformed regime [19,32].

The obtained data enable a better understanding of the D_1 sinistral transpressive regime, emphasising both the importance of strain partitioning and of distinct folding mechanisms in the course of the first phase of Variscan deformation. This will also contribute to the knowledge of the geodynamic evolution of the Ibero-Armorican Arc.

2. Geological setting

Previous works [6,36,37] have shown that the Torre de Moncorvo region (Fig. 1) is fundamental to the understanding of the early Variscan deformation in the Autochthon Domain of the Iberian Terrane in Portugal. Here, the most conspicuous structures are attributed to the first Variscan

* Corresponding author.
E-mail address: rdias@uevora.pt (R. Dias).

Published by Éditions scientifiques et médicales Elsevier SAS.
doi:10.1016/j.geoact.2003.04.001

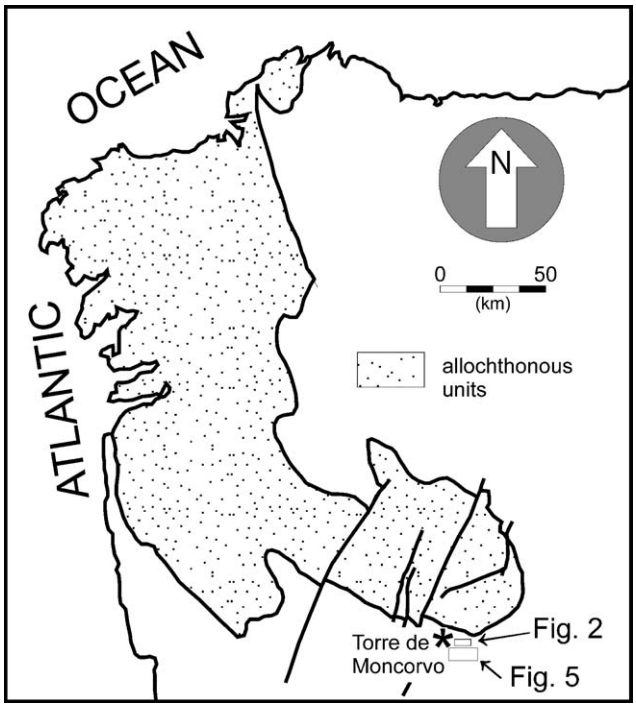

Fig. 1. The study areas and the NW Iberian allochthonous terranes (adapted from [34]); the location of Figs. 2 and 6 are shown.

tectonic event (D_1) of the Upper Devonian age, although specific features created by local tectonic overprinting can be recognised, both near the tectonic contacts with the Allochthonous Units of NW Iberian and with the adjoining post-collisional granitic batholiths. Away from these particular areas, large-scale shear zones subparallel to major D_1 folds are well preserved [6,7,37], recording a sinistral transpressive regime induced by the development of the Ibero-Armorican Arc [9,10,38].

Like in most of the northern Portugal autochthon, the major framework of the two studied sectors (Souto da Velha and Torre de Moncorvo syncline) are due to the D_1 Variscan deformation phase. The related structures are well preserved in the metasedimentary sequence of Ordovician age, which is considered the stratigraphic equivalent of the Armorican Quartzites identified in the northern branch of the Ibero-Armorican Arc [37]. The D_1 cylindrical folds, with an approximate E–W trend (Fig. 2A), always contain a pervasive S_1 cleavage (Fig. 2B) that can transpose the bedding planes when the slaty component becomes predominant. Frequently, this transposition generates quartzitic mullion structures (Fig. 2E) subparallel to the fold axes.

Most of the times, the bedding–cleavage intersection (L_1; Fig. 2C) presents a low dip (less than 20°), being subparallel to the D_1 fold axes; this relation suggests that there is no transection at a regional scale. Nevertheless, the quartzitic layers of some mesoscopic folds of the Souto da Velha sector (Fig. 2) present a slightly clockwise-rotated cleavage that is spatially related to smaller folds with an axial plane cleavage (Fig. 3), which is a common situation in transection geometry [31]. This transection is only found locally in the quartzites, whereas in the interbeded slaty horizons the intersection lineation is always parallel to the fold axes [6]. Similar features were already described for Silurian pelitic rocks in New Brunswick, Canada [1], and provide several lines of evidence for the prevailing (inter- or intragranular) mechanisms of strain accommodation at grain-scale. Given the mineralogical and textural characteristics of the deformed metasedimentary sequence, it is plausible to consider that cleavage development in the slaty layers are always coeval with the beginning of the folding processes, while in the quartzitic layer it could represent a slightly later time. Under a non-coaxial regime, the cleavage in the quartzites could be oblique to the axial plane, because it was overprinted in slightly older folds [31]. The relative importance of this sinistral shear component during the first Variscan deformation phase was already distinguished in other regions of northern Portugal [7,9,37]. In the Souto da Velha sector three steeply dipping major sinistral shear zones have been mapped, with a general command almost parallel to the main D_1 folds. These zones are usually underlined by discontinuous metric-thick quartz veins, whose boudinage is fully coherent with the X_1 sub-horizontal stretching lineation (Fig. 2D).

Any attempt to integrate all the above characteristics indicates a sinistral transpressive regime. The close parallelism between the D_1 axial planes and the shear zones implies either an infinite simple shear or a transpressive regime [41]. This problem is very similar to the one characterised by Sanderson [40] in Brittany. It was recently pointed out by several authors studying transpressive wrench tectonics, that there was a crucial role for partitioning the fault motions, with the purely shortening structures largely decoupled from the strike–slip faults [2,13,15,16,21,23,28,39,42,43]. This explains the parallelism between the D_1 folds and shear zones at the Souto da Velha sector, where the sinistral simple shear component is concentrated along the major steeply dipping structural corridors.

3. Finite strain analysis

In order to estimate the finite strain, we used different strain markers in Ordovician and Silurian rocks. As we have obtained strain ellipsoids using different rocks and methods, some conclusions can be drawn concerning strain partitioning of the Variscan deformation in the Centro-Iberian autochthon.

3.1. Strain markers

In autochthonous northern Portugal, the most suitable material for strain studies are the Armorican Quartzites [7] of Lower Ordovician age [35]. The quartzites are widely distributed and are very pure, consisting almost entirely of quartz grains, in which the undulose extinction is frequent but the subgranulation and the recrystallisation phenomena have only a localised development. In these rocks, we were

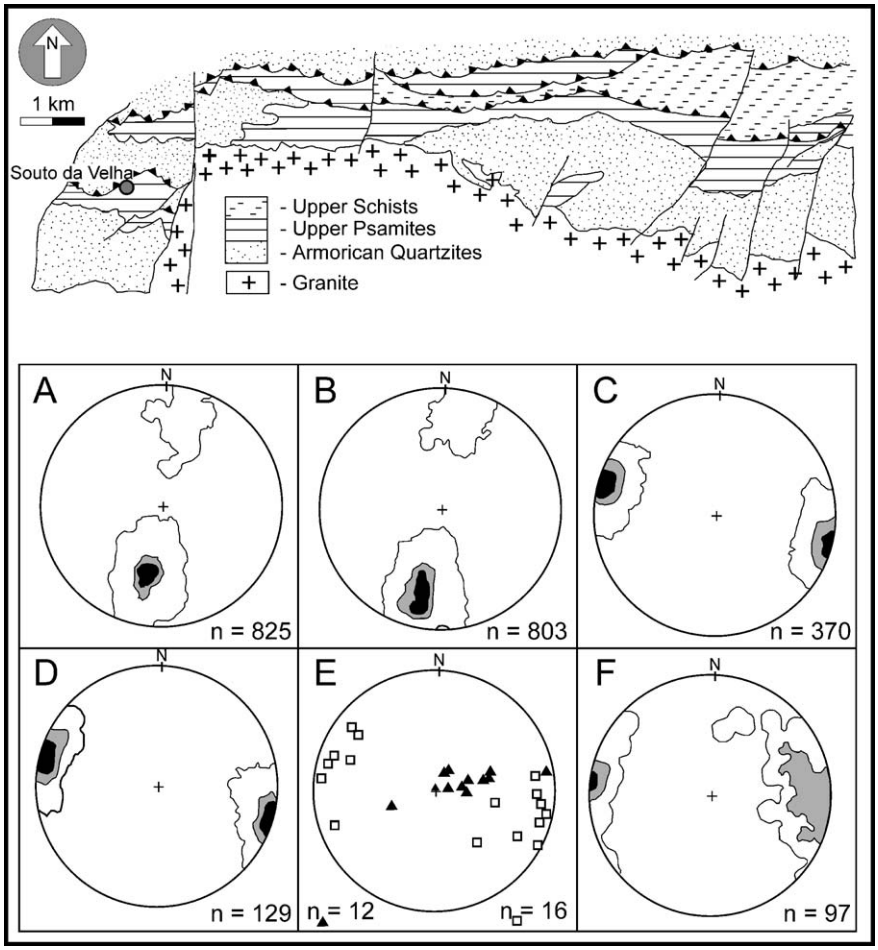

Fig. 2. Geological map of Souto da Velha sector and contoured equal area lower hemisphere stereographic projection of some related D_1 structures. (A) S_0 (1%, 8%, 12%); (B) S_1 (1%, 7%, 11%); (C) L_1 (2%, 20%, 40%); (D) X_1 (2%, 20%, 40%); (E) Mullions (squares) and boudins (triangles); (F) *Skolithos* (1%, 22%, 30%).

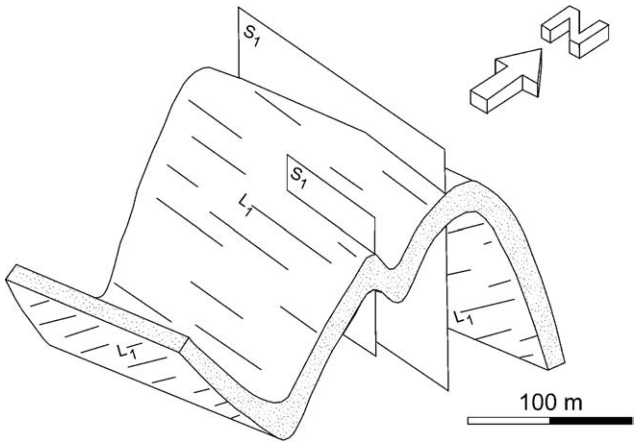

Fig. 3. Geometrical relation between major and minor D_1 Variscan folds and related cleavage.

able to estimate the strain using two kinds of strain markers: the detrital quartz grains and the worm burrows *Skolithos*.

We have also estimated the strain using well-sorted oolitic ironstones of Upper Ordovician/Lower Silurian age [35]. In the low strained samples, the oolites are isolated and pressure-solution is very weakly developed; at higher strains the oolites begin to touch each other along pressure-solution surfaces. Nevertheless, it was always possible to identify the particle centres because of the concentric nature of most oolites. In most of the samples, the pressure-solution surfaces are closely spaced and the local precipitation phenomena are rare. According to Onasch [29] classification, the deformation of this material is described as homogeneous pressure-solution with volume loss.

3.2. Methodologies

We have used two methods to estimate the three-dimensional strain. For the *Skolithos*, we have applied the method proposed by Dias and Ribeiro [8], which combines the rotation of the worm tubes, with their intersections in the bedding plane. This method is an improvement of Paulis' [30], which only uses the deflection of the tubes, and can be used where there is no rheological contrast between the material inside and outside the tubes.

When studying the detrital quartz grains or the oolitic particles, in order to estimate the strain ellipsoid, we used

three subperpendicular thin sections for each sample. In these sections, we applied the normalised Fry method [12] as a measure of the strain magnitude. In the Armorican Quartzites of the Centro-Iberian autochthon, this method proved to be more suitable than the Rf/Ø method or the classical Fry method, to estimate the overall rock deformation [14]. The two-dimensional strain data of the three subperpendicular thin sections were combined using the method proposed by De Paor [4].

3.3. Strain ellipsoid data

3.3.1. Strain ellipsoid shape

Using the *Skolithos* field data (Table 1), we have been able to estimate the strain ellipsoids at six locations (Table 2), which can be visualised (Fig. 5) in a Ramsay logarithmic plot [33]. Here the mean strain ellipsoid for these data is also shown, which has been estimated using the weighted mean centre technique [11].

The mean ellipsoid has a slightly prolate shape, falling not very far from the plane strain line; this situation has already been described as typical for the northern Portugal autochthon [9]. Only two oblate ellipsoids were found in the short limb of a second order antiform. In the Torre de Moncorvo region, this tendency towards less constriction in local second order short limbs has already been found [9].

The Armorican Quartzites have also been sampled to estimate the strain using Fry on detrital quartz grains, which allows us to have a more pervasive distribution of the strain data. We have sampled both limbs of the Torre de Moncorvo syncline (Fig. 5, samples Mv1–Mv7) as well as two mesoscopic folds in the Souto da Velha region (Fig. 6, samples Mv8–Mv11).

The strain ellipsoids estimated using the quartz grains (Table 3 and Fig. 7) are similar to those obtained by the *Skolithos* method. We usually get constrictional forms, with rare slightly oblate ellipsoids. For the Souto da Velha data, the mean strain ellipsoid is slightly more prolate than the one

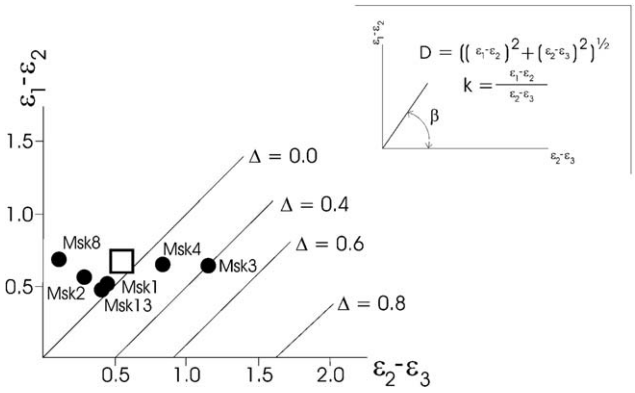

Fig. 4. Ramsay logarithmic plot for the finite strain ellipsoids obtained using *Skolithos* of Torre de Moncorvo syncline; the inset shows the strain parameters used in this work (according to [30]). The square represents the mean strain ellipsoids for these data.

of the Torre de Moncorvo syncline (*K* parameter of 2.14 vs. 1.33). Comparing the *D* parameter for these ellipsoids (respectively, 0.25 and 0.16), we get higher values for the Souto da Velha area. As both ellipsoids have comparable *K* values, the *D* parameter could be used as a measure of strain intensity [33], which seems to indicate that the samples of the Torre de Moncorvo syncline are slightly less deformed than the others.

When comparing the strain intensities obtained using the *Skolithos* and the detrital quartz grains, some discrepancies become evident. As both mean ellipsoids present similar mean *K* values (1.15 and 1.33), we can also use the *D* parameter as a measure of the strain intensity; the *Skolithos* value (0.77) indicates a much higher strain intensity than the quartz grains one (0.16). This difference is related to the fact that either the deflection of the worm tubes, or the distortion of their intersections with the bedding plane are sensitive, both to intragranular and intergranular deformation mechanisms. The Fry methodology mainly reflects the intragranular processes, being insensitive to most of the rearrangements along the grain boundaries [33]. Thus, the *Skolithos* values

Table 1
Skolithos field data

Sample	S_0	S_1	$L_1(S_0\text{^}S_1)$	X_1	*Skolithos*	*a/b*
Msk1	N59°E,39°E	N65°W,81°N	32°,S68°E	32°,S68°E	27°,N54°W	2.3
Msk2	N47°E,38°E	N81°W,81°S	34°,S75°E	34°,S75°E	26°,N66°W	2.1
Msk3	N80°W,86°N	N85°W,57°S	19°,S79°E	35°,S61°E	47°,S32°E	1.7
Msk4	N82°W,81°S	N84°W,54°S	1°,S80°E	20°,S68°E	32°,S30°E	–
Msk8	N75°W,62°N	N77°W,33°S	4°,S81°E	11°,S66°E	30°,S20°E	2.0
Msk13	N57°E,37°N	N86°W,51°S	15°,S88°E	3°,S84°E	28°,S55°E	2.2

Table 2
Skolithos strain ellipsoid parameters

Sample	*X/Y*	*X/Z*	*Y/Z*	Ellipsoid	*K*	*β*	*D*
Msk1	1.6	2.3	1.5	1.6:1:0.7	1.18	49°	0.62
Msk2	1.7	2.2	1.3	1.7:1:0.8	2.04	64°	0.59
Msk3	1.9	5.2	3.0	1.9:1:0.3	0.58	30°	1.27
Msk4	1.9	4.3	2.2	1.9:1:0.4	0.82	39°	1.02
Msk8	2.0	–	1.1	2.0:1:0.9	7.27	82°	0.70
Msk13	1.6	–	1.5	1.6:1:0.7	1.16	49°	0.62

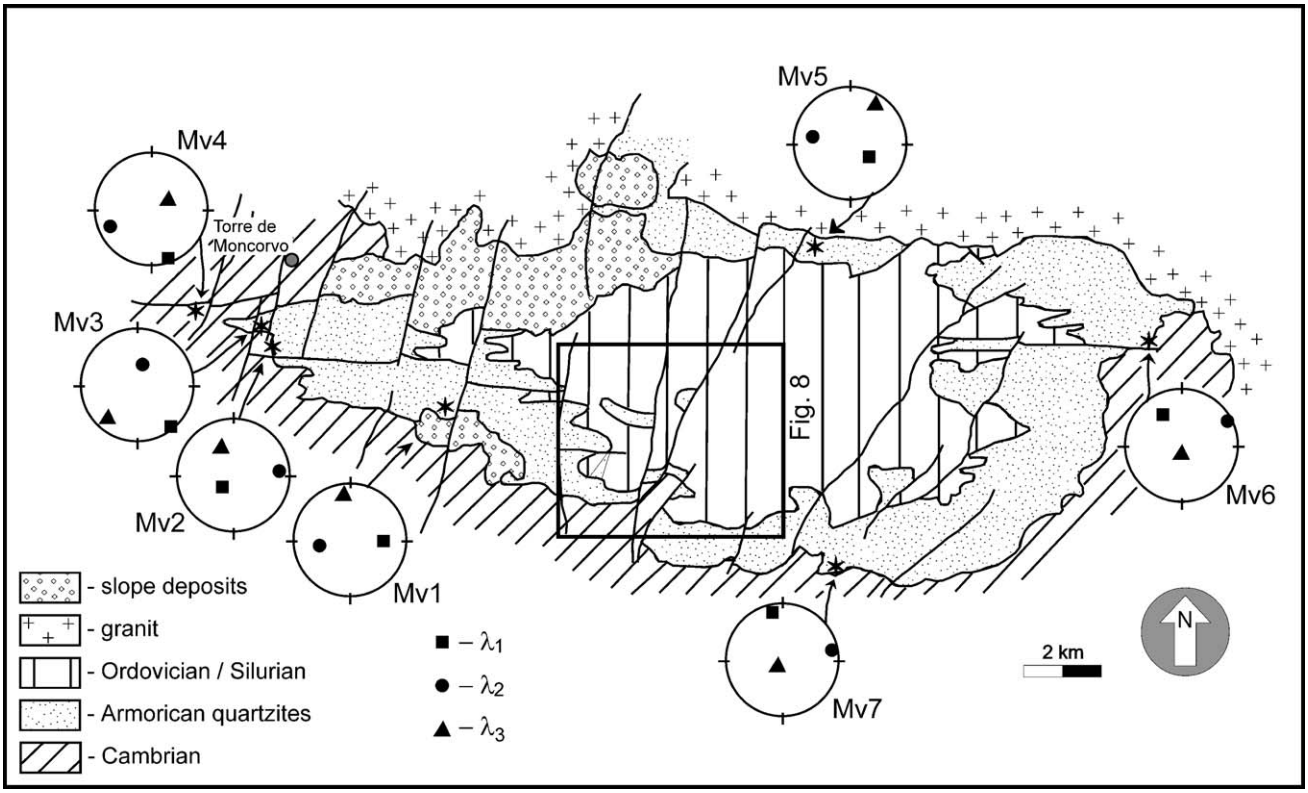

Fig. 5. Simplified Torre de Moncorvo syncline mapping with the finite strain ellipsoids orientations and the location of Fig. 14.

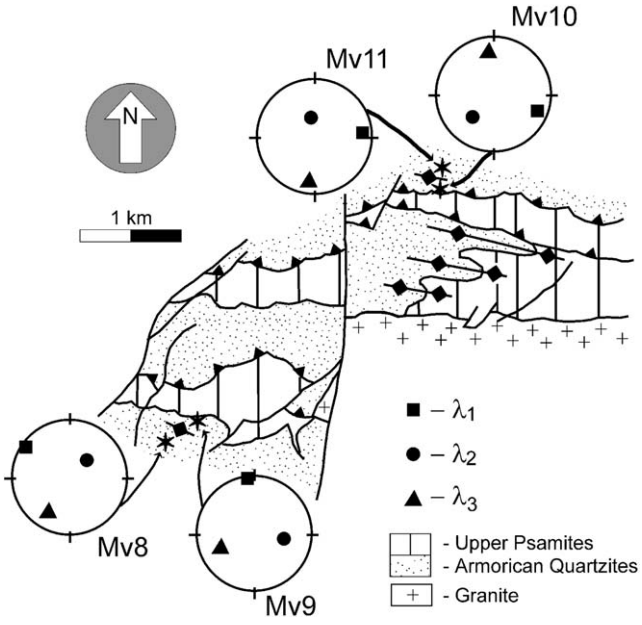

Fig. 6. Simplified Souto da Velha mapping with the finite strain ellipsoids orientations.

Table 3
Strain ellipsoid parameters obtained using detrital quartz grains

Sample	λ_1	λ_2	λ_3	Ellipsoid	K	β	D
Mv1	1.3	1.0	0.8	1.3:1:0.8	1.18	50°	0.17
Mv2	1.2	1.0	0.8	1.2:1:0.8	0.82	39°	0.14
Mv3	1.2	1.0	0.8	1.2:1:0.8	0.82	39°	0.14
Mv4	1.4	0.9	0.8	1.6:1:0.9	3.75	75°	0.23
Mv5	1.3	1.0	0.8	1.3:1:0.8	1.18	50°	0.17
Mv6	1.2	1.0	0.9	1.2:1:0.9	1.73	60°	0.11
Mv7	1.3	1.0	0.8	1.3:1:0.8	1.18	50°	0.17
Mv8	1.8	0.9	0.6	2.0:1:0.7	1.73	60°	0.40
Mv9	1.6	0.8	0.8	2.0:1:1.0	+∞	90°	0.35
Mv10	1.2	1.0	0.9	1.2:1:0.9	1.73	60°	0.11
Mv11	1.3	1.0	0.7	1.3:1:0.7	0.74	36°	0.22

are closer to the bulk strain intensity of the deformed quartzites. Nevertheless, the estimated K parameters for both mean ellipsoids are similar, consequently different deformation mechanisms give rise to different measured finite strain magnitudes. The shape of the estimated strain ellipsoids is also similar (e.g. [22]).

In the core of the Moncorvo syncline, Lower Silurian rocks are preserved in second order synclines. The transition from the Ordovician to the Silurian is underlined by discontinuous oolitic ironstones and limestone layers [35]. Outcrops where the oolites are best preserved have been sampled for strain studies (Fig. 8) using the same method as for the detrital quartz grains.

The strain ellipsoids of the oolitic ironstones (Table 4 and Fig. 9) fall close to the plane strain line. Nevertheless the oblate forms are predominant. This tendency towards apparent flattening contradicts what is known for this region (Figs. 4 and 7), dominated by constriction regime [7,9]. However, this discrepancy disappears when the pressure-solution phenomena are taken into account [34]. As was previously mentioned, the oolitic ironstones show a perva-

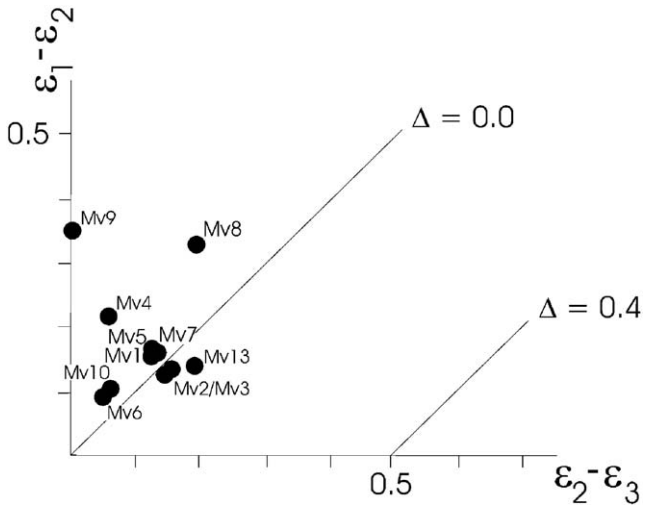

Fig. 7. Ramsay logarithmic plot for the finite strain ellipsoids obtained using detrital quartz grains of Torre de Moncorvo syncline and Souto da Velha sectors.

Table 4
Strain ellipsoid parameters obtained using oolithic ironstones

Sample	λ_1	λ_2	λ_3	Ellipsoid	K	β	D
2028	1.6	1.0	0.6	1.6:1:0.6	0.92	43°	0.35
2029	1.8	1.4	0.4	1.3:1:0.3	0.20	11°	0.64
3076	2.0	1.0	0.5	2.1:1:0.5	1.00	45°	0.49
3123	1.2	1.0	0.8	1.2:1:0.8	0.82	39°	0.14
3136	1.7	0.9	0.6	1.9:1:0.7	1.57	58°	0.38
3137	1.5	1.0	0.6	1.5:1:0.6	0.79	38°	0.33
3176	1.5	0.9	0.7	1.7:1:0.8	2.03	64°	0.28
3177	1.4	1.1	0.6	1.3:1:0.6	0.40	22°	0.33

sive and intense pressure-solution effect. So, if one considers that during the Variscan deformation a 10–20% of diagenic volume loss occurred, most of the strain ellipsoids are indeed constrictional (Fig. 9), similar to the ones in the Armorican Quartzites.

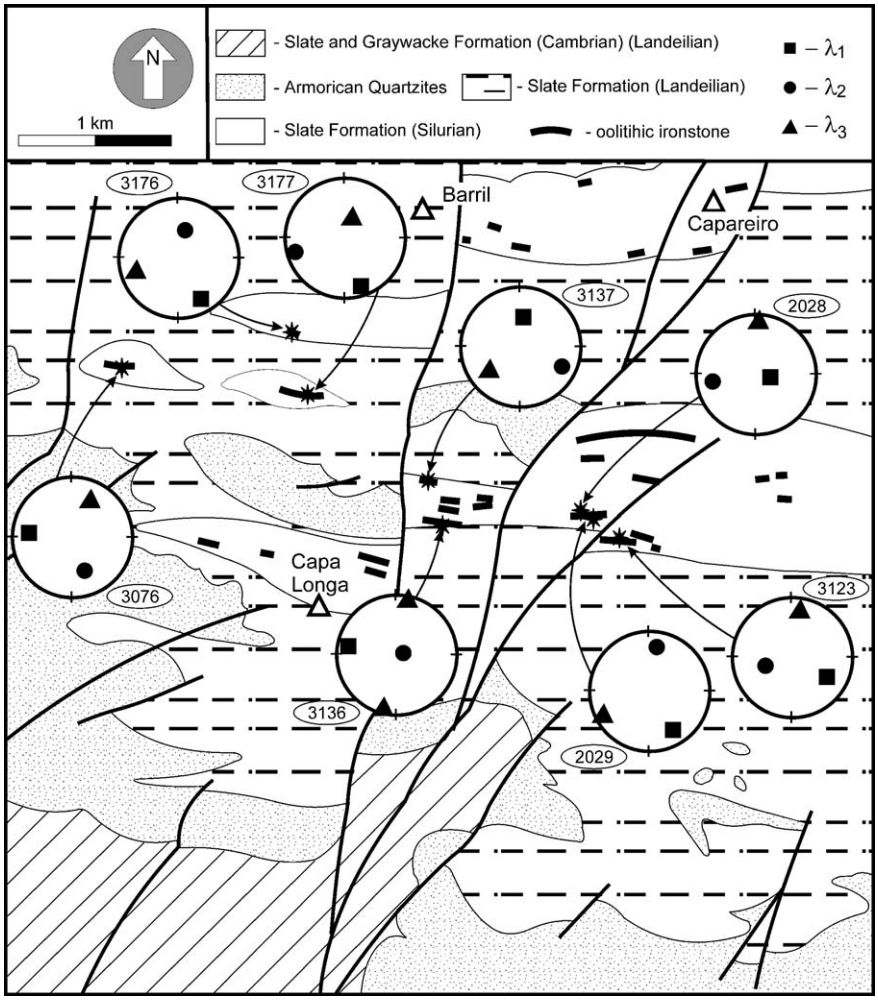

Fig. 8. Simplified geological mapping of the southwest area of the Torre de Moncorvo syncline core, showing the strain ellipsoids orientations obtained using oolithes as strain markers.

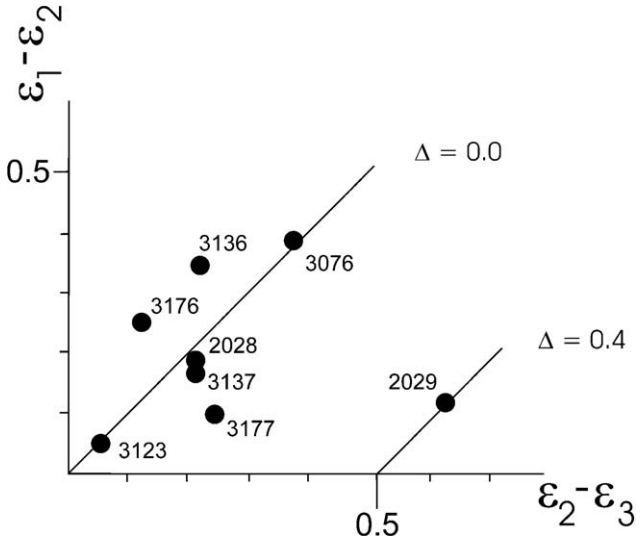

Fig. 9. Ramsay logarithmic plot for the strain ellipsoids obtained using oolithic ironstones of Torre de Moncorvo region.

3.3.2. Strain ellipsoid orientation

Concerning the strain ellipsoid orientation, we are mainly discussing the data obtained using the Fry method because the *Skolithos* method gives no independent way to estimate the orientation of the strain ellipsoid [8,30].

From the strain ellipsoid orientations (Tables 5 and 6; Figs. 6 and 7) and their geometrical relation with the Variscan D_1 folds, some aspects can be emphasised. Concerning the minor axis (λ_3) attitude, its direction is often subperpendicular to the E–W structural trend, or presents a frequent clockwise rotation. The previous geometrical relations agree, either with strong strain partitioning, or with the transection locally found in this region. The transection can be easily explained if we admit that the observed intergranular fracture mechanism is predominant during the earlier stages of the deformation. The layers began to develop en echelon folds (Fig. 10A) but the shape of the detrital quartz did not change. The Fry method is unable to estimate the finite strain in such cases [33]. With the increasing deformation (Fig. 10B), the previously developed folds rotate towards the shear zone boundaries. In this intermediate stage, the intragranular deformation mechanisms become active, developing strain ellipses from the shape of the detrital quartz grains, which do not reflect the bulk strain of the rock. As the folds suffer most of the progressive deformation, while the strain ellipse is only sensitive to part of it, an obliquity between both was developed. With the increase of the deformation (Fig. 10C), not only the folds but also the strain ellipse major axis rotate towards the boundaries of the shear zone [45].

Table 5
Strain ellipsoid orientations using detrital quartz grains

Sample	λ_1	λ_2	λ_3
Mv1	36°,S86°E	52°,S76°W	10°,N3°W
Mv2	71°,S37°W	12°,N81°E	48°,N25°W
Mv3	16°,S47°E	57°,N19°E	31°,S43°W
Mv4	4°,S24°E	30°,S69°W	60°,N60°E
Mv5	57°,S62°E	32°,N74°W	20°,N28°E
Mv6	42°,N30°W	2°,N62°E	80°,S7°E
Mv7	8°,N13°W	6°,N77°E	81°,S31°W
Mv8	6°,N52°W	56°,N49°E	34°,S31°W
Mv9	11°,N8°W	52°,S82°E	34°,S60°W
Mv10	15°,S71°E	55°,S42°W	27°,N2°W
Mv11	1°,E	66°,N1°E	25°,S3°W

Table 6
Strain ellipsoid orientations using oolithic ironstones

Sample	λ_1	λ_2	λ_3
2028	60°,S70°E	26°,S81°W	14°,N3°W
2029	20°,S35°W	23°,N12°E	17°,S60°W
3076	22°,N85°W	44°,S18°E	39°,N24°E
3123	34°,S68°E	49°,S73°W	20°,N8°E
3136	11°,N82°W	79°,S82°E	0°,N10°E
3137	55°,N11°E	14°,S60°E	33°,S40°W
3176	22°,S32°E	55°,N22°E	26°,S67°W
3177	16°,S20°E	14°,S75°W	60°,N20°E

In a homogeneous transpressive regime, the obliquity between the folds, the strain ellipsoid minor axes and the shear zone boundary greatly depends on the relative role of the simple shear and pure shear components [41,42,45]. However, in more complex heterogeneous transpressive regimes, the previous geometrical relations are greatly dependent on the degree of partitioning between these shear components [13,21,28,39,42,43]. In a wrench dominated transpressive regime [13], with lateral escape, as was proposed to this region [9], all the structures tend to become subparallel.

Concerning the major axes of the finite strain ellipsoids, their geometrical relation with the fold axes is not a simple one. When comparing their attitudes, a complex pattern becomes evident. Indeed, if in some cases they are subparallel, a high obliquity is also frequent, which easily attains values close to 90°. These different geometrical relations could be explained by differences in the folding mechanisms, as it has been found in other places of the Centro-Iberian autochthon [7]. The strain pattern in a fold generated in a transpressive regime may be highly heterogeneous, due to the factorisation of the transpression into two nearly independent components. Some domains can be mainly affected by contraction subperpendicular to the structures, while in others, the regional strike–slip component could predominate. A similar

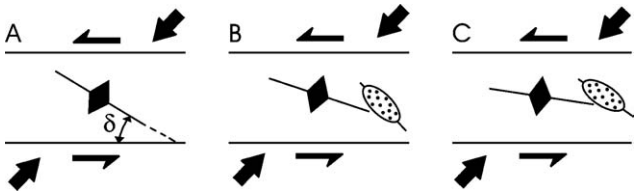

Fig. 10. Sketch of a sinistral transpressive shear zone affected by progressive deformation: (A) earlier stage where the intergranular deformation mechanisms predominate, giving rise to oblique fold axes; (B) intermediate stage where the intergranular phenomena began to be active; (C) final stage, where both the fold axis and the strain ellipse have been rotated towards the shear zone boundary.

behaviour has been proposed based either on field evidence in the San Andreas region [28,42] or on experimental work [39].

4. Folding mechanisms

The existence of *Skolithos* in strained materials gives useful indications for the understanding of the deformation mechanisms that have been active [8]. Although in the Armorican Quartzites of Torre de Moncorvo these worm tubes are not frequent, their study proves to be a powerful tool not only in estimating the finite strain but also as an indication of the shear movement. When combining this shear sense data with the three-dimensional finite strain pattern some constrains can be put in the folding mechanisms that have been active.

In the undeformed state the *Skolithos* are straight, cylindrical to subcylindrical tubes that lie more or less perpendicular to the bedding surface [3,27]. Thus, the deflection of these worm tubes away from the perpendicularity to the bedding plane can give useful indication about the shear movements occurred [8]. However, McLeish [26] noted that *Skolithos* are not always perpendicular to the layers in their undeformed state; in some less deformed outcrops he found tubes lying at a variety of angles to the bedding. In the Torre de Moncorvo region, we also found some outcrops where the worm tubes present a reasonable dispersion. Nevertheless, this is not a problem in their use in kinematic studies, because when working with the median of the population, the shear sense becomes clear [8].

Along the Torre de Moncorvo syncline, the geometrical relations between the *Skolithos* and the bedding plane are strongly different from limb to limb. When the layers dip to south, the worm tubes are deflected towards northwest. In contrast, when the beds are subvertical or have a northern dip, the *Skolithos* were deflected towards southeast (Table 1). As pointed out by Dias and Ribeiro [8], this behaviour is impossible to explain if one considers that only tangential longitudinal strain or flexural flow generated the folds. However, if we consider a sinistral transpressive regime [6,37], the geometries of the *Skolithos* can be explained by a combination of flexural flow and the regional wrench component (Fig. 11) typical of the south branch of the Ibero-Armorican Arc [10,25].

In the Souto da Velha sector, these worm tubes have only been found in the centimetric alternation of light quartzites and dark slaty layers that made the transition to the Upper Ordovician schists. There they appear as quartzitic tubes in a more pelitic matrix. However, due to extreme ductility contrast problems, they have been strongly deflected away from the perpendicular onto the bedding plane, becoming subparallel to the X_1 stretching lineation. Although there are no strain values for this transition formation, the above geometrical relations show that it was much more deformed during the Variscan orogeny than the Armorican Quartzites.

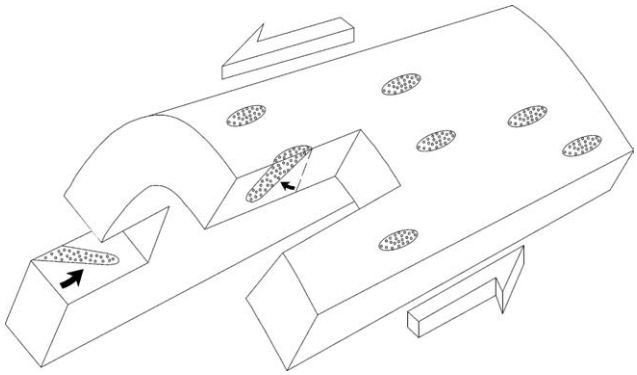

Fig. 11. *Skolithos* behaviour in parallel folds induced by flexural flow and regional sinistral shear (adapted from [7]).

The *Skolithos* observations allow the improvement of the three-dimensional theoretical models for strain pattern in folds due to different folding mechanisms. Previous models [18,47] are rare (Fig. 12A,B) and inadequate to explain transpressive-generated folds. For folds developed by transpression, we can infer a possible strain pattern combining flexural shear, due to the folding process, with sinistral shear induced by the regional tectonic setting (Fig. 12C). The reason for choosing a flexural shear component is because previous works [6,7] have shown that flexural shear must be an active mechanism in the Ordovician quartzitic layers of the Torre de Moncorvo region during the formation of the D_1 Variscan folds. Several lines of evidence suggest that:

- the *Skolithos* in the fold limbs are deflected from the perpendicular to the bedding [8];
- in the bedding plane it is frequent to find slickensides lineations;
- in some layers the S_1 cleavage is distorted sigmoidally, showing that the bedding plane has been kinematically active during folding process.

The predicted model is only one of the possible combinations and does not mean that in folded multilayers several of the previous mechanisms could not coexist along the same fold [24]. So, a wide range of major strain axes orientation could be expected. The diversity depends on the:

- folding mechanisms that were active;
- exact position of the sample in the folded layer (e.g. below or above the neutral surface, if this exist; Fig. 12A);
- degree of partitioning between the simple shear and the pure shear components.

In the Torre de Moncorvo region, we have sampled both limbs of several hectometric D_1 folds in order to have an idea of how the deformations have been accommodated during Variscan folding. With only one sample in each limb, it is not possible to reach only one solution. Nevertheless, the obtained data allows us to constrain the possible solutions.

In the first case we have studied a fold located 3 km southwest of Moncorvo (Fig. 5). On both limbs, we have estimated the orientation of major strain axes using a normalised Fry method in detrital quartz grains (samples Mv2 and Mv3). Moreover, we also have been able to identify a sinis-

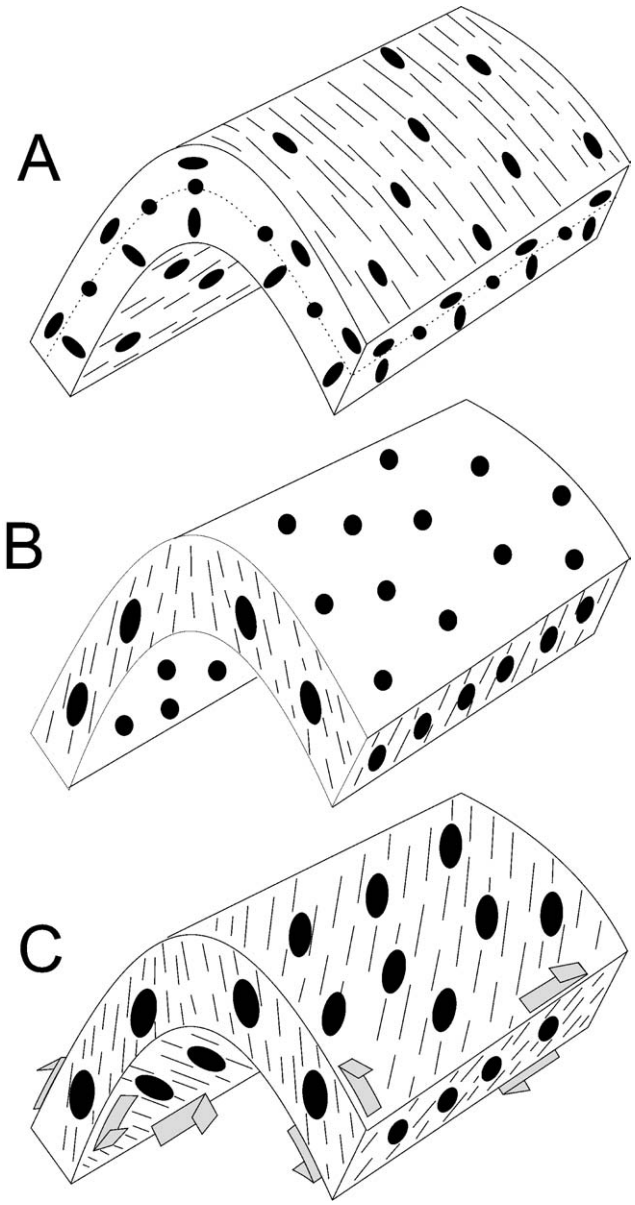

Fig. 12. Three-dimensional strain pattern in a fold due to: (A) orthogonal flexure (adapted from [16]); (B) flexural shear (adapt. from [16]); (C) flexural shear plus sinistral shear.

tral shear sense along each limb using the *Skolithos* attitudes (Msk1, Msk2, Msk3 and Msk4). All these geometrical features are sketched in Fig. 11. Comparing these data with the developed theoretical models (Fig. 13), we see that they are compatible with flexural shear combined with a regional sinistral shear.

The second fold studied (Mv8 and Mv9) and is located near the Souto da Velha (Fig. 6). The relation between the major strain axes and the fold is completely different here (Fig. 14). In the short limb the major axis is subparallel to the fold axis, while in the long limb it is almost perpendicular. These orientations are unexpected if we use the flexural shear plus sinistral shear model. However, this strain geometry is compatible with a fold developed by orthogonal flexure; the

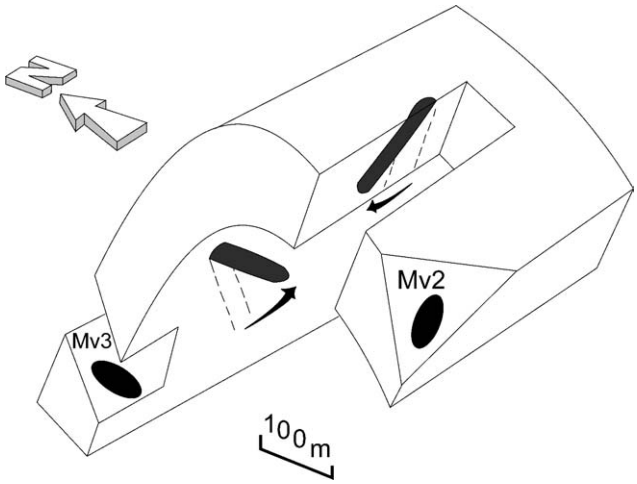

Fig. 13. Sketch of the geometrical relations between *Skolithos* (in grey) and major strain axes (shown by the black ellipses) around a mesoscopic fold near Torre de Moncorvo.

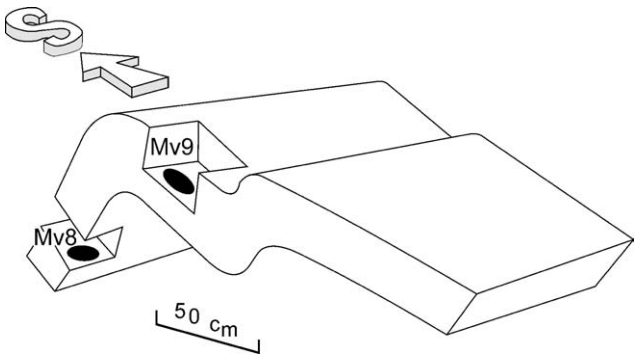

Fig. 14. Sketch of the behaviour of major strain axes (shown by the black ellipses) around a mesoscopic fold near the Souto da Velha wrench fault.

Mv8 should be a sample taken below the neutral surface, while the Mv9 was taken above the neutral surface.

When trying to make the pervasive regional sinistral transpressive regime compatible with folds developed by an almost pure orthogonal flexure mechanism, an important strain-partitioning component is inescapable. In such a situation, the sinistral shear component is strongly concentrated along the wrench faults, while the pure shear component was related to coeval folds [13,28,42,43]. In our case, close to the studied fold, a major D_1 sinistral strike–slip fault (the Souto da Velha one; Fig. 6) was put in evidence [6,7].

The third fold that was studied (Mv10 and Mv11) is also located near the Souto da Velha (Fig. 6). In both limbs, the major strain axes are subparallel to the fold axis (Fig. 15). This geometrical relation is compatible with the orthogonal flexure if the two samples were taken below the neutral surface. In this example, the strain partitioning must also have been important, which should be related to the vicinity of the important Ribeira do Inferno sinistral strike–slip shear zone (Figs. 6 and 15; [6]).

The available data indicate that in the Souto da Velha region the strain partitioning was very important during Variscan times. This important strain partitioning explains

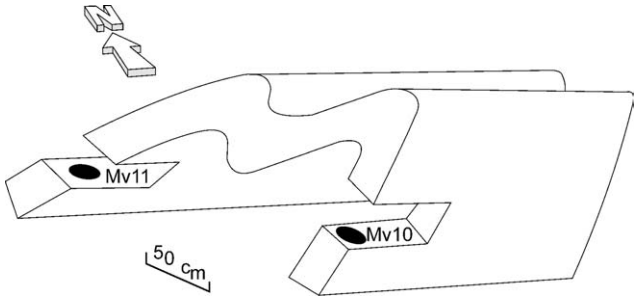

Fig. 15. Sketch of the behaviour of major strain axes (shown by the black ellipses) around a mesoscopic fold near the Ribeira do Inferno wrench fault.

why the fold trends are subparallel to the major faults in the northern part of the Centro-Iberian Variscan autochthon. Inside the domains bounded by the major wrench faults a pure shear dominated transpression predominates. It changes into a simple shear dominated transpression along the major sinistral shears.

Concerning the orientation of the strain ellipsoids estimated for the oolitic ironstone samples (Fig. 8 and Table 6), we get results similar to those obtained for the quartz grains.

The geometrical behaviour of the major strain axes is easily understood using the theoretical structural models previously outlined. Moreover, with the oolitic data, these axes are shown to be either subparallel, oblique or subperpendicular to the fold axes. In most cases, we are dealing with samples of the reverse limb in which the major strain axes plunge towards southeast (samples 2028, 2029, 3123, 3176 and 3177). As already mentioned, this is what should be expected using a model combining flexural shear induced by the folding mechanism, with sinistral shear due to the regional tectonic setting (Fig. 16A). The same model may explain the behaviour of sample 3076; indeed, now we are in a long limb situation and the major strain axis slightly plunges in a northwest heading.

Concerning the samples 3136 and 3137, the pattern of the major axes of the strain ellipsoid around the fold is explained if the orthogonal flexure has been the predominant folding mechanism. In this situation the long limb sample (3137) should be located below the neutral surface, while the reverse limb sample (3136) must be above the same surface (Fig. 16B).

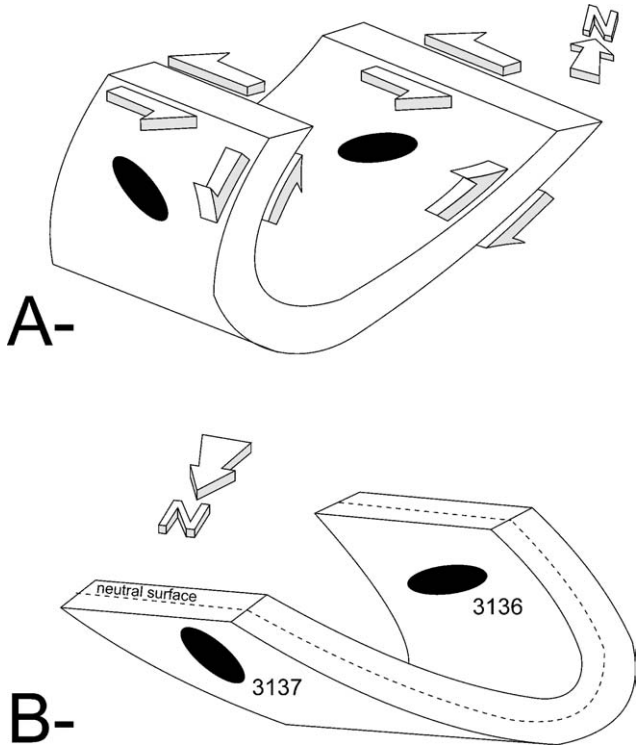

Fig. 16. Sketch of the Torre de Moncorvo second order synclines, showing the behaviour of major strain axes, when these folds are due to: (A) orthogonal flexure; (B) flexural shear plus sinistral shear.

5. Conclusions

In the Torre de Moncorvo region several methods of finite strain measurements show that slightly prolate strain ellipsoids are predominant. The fact that the Variscan deformation in this region was transpressive [6,37] confirms the association of such a deformation regime with the constriction strain ellipsoids [9].

Strain studies in this region also show that the strain partitioning may be very important in regions where the transpression deformation is predominant. The decoupling of two components (a simple shear and a pure shear) induced the coexistence of different folding mechanisms in the same area. As nearly identical fold profiles can be achieved by different deformation mechanisms [18,19,47], geometrical studies alone are incomplete for the understanding of the tectonic evolution. However, when combined with quantitative strain estimations, we get a powerful tool for the study of the regions deformed by transpression.

Acknowledgements

This work was carried out with the financial support of the JNICT through the grant REDIBER—PBICT/P/CTA/2113/95 and LATTEX, PRAXIS XXI, project 125/N/92. This is a work of the TEKTONIKOS (Experimental Tectonic and Microtectonic Laboratory of the Évora University). A thorough review by Basil Tikoff greatly helped clarify some of the issues contained herein. Some comments of R. Lisle and J. Burg on an early version of this paper were also a valuable contribution for our ideas. We also want to thank José Rebelo for helpful advice during fieldwork.

References

[1] G. Borradaile, Transected folds: a study illustrated with examples from Canada and Scotland, Geol. Soc. Am. Bull. 89 (1978) 481–493.
[2] C. Coke, R. Dias, A. Ribeiro, Rheologically induced structural anomalies in transpressive regimes, J. Struct. Geol. 25 (3) (2003) 409–420.

[3] T. Crimes, The stratigraphical significance of trace fossils, in: R.W. Frey (Ed.), The Study of Trace Fossils, Springer, New York, 1975, pp. 109–130.
[4] D. De Paor, Determination of the strain ellipsoid from sectional data, J. Struct. Geol. 12 (1990) 131–137.
[5] J. Dewey, R. Holdsworth, R. Strachan, Transpression and transtension zones, in: R. Holdsworth, R. Dewey, J. Strachan (Eds.), Continental Transpression and Transtension Tectonics, Geol. Soc., 135, 1998, pp. 1–14.
[6] R. Dias, Estudo de um sector do autóctone de Trás-os-Montes oriental a ENE de Torre de Moncorvo, M. Sci. Thesis, Lisbon University, 1986 153 pp.
[7] R. Dias, Regimes de deformação no autóctone da zona Centro-Ibérica: importância para a compreensão da génese do Arco Ibero-Armoricano, Ph. D. Thesis, Lisbon University, 1994.
[8] R. Dias, A. Ribeiro, Finite strain analysis in a transpressive regime (Variscan autochthon, northeast Portugal), Tectonophysics 191 (1991) 389–397.
[9] R. Dias, A. Ribeiro, Constriction in a transpressive regime: an example in the Ibero-Armoricain, Arc. J. Struct. Geol. 16 (11) (1994) 1543–1554.
[10] R. Dias, A. Ribeiro, The Ibero-Armorican Arc: a collisional effect against an irregular continent? Tectonophysics 246 (1995) 113–128.
[11] D. Ebdon, Statistics in Geography, Basil Blackwell, Oxford, 1977, pp. 195.
[12] E. Erslev, Normalized center-to-center strain analysis of packed aggregates, J. Struct. Geol. 10 (1988) 201–209.
[13] H. Fossen, B. Tikoff, C. Teyssier, Strain modeling of transpressional and transtensional deformation, Norsk Geologisk Tidsskrift 74 (1994) 134–145.
[14] C. Garcia, S. Machado, R. Dias, C. Coke, A. Ribeiro, Comparison of methods of finite strain analysis in the Buçaco region (Centro-Iberion Zone): Tectonic implications, Comun. "XII Reunião de Geologia do Oeste Peninsular", Évora, Portugal, 1993, pp. 65–76.
[15] F. Gomez, R. Allmendinger, M. Barazangi, A. Er-Raji, M. Dahmani, Crustal shortening and vertical strain partitioning in the Middle Atlas Mountains of Morocco, Tectonics 17 (4) (1998) 520–533.
[16] L. Goodwin, P. Williams, Deformation path partitioning within a transpressive shear zone, Marble Cove, Newfoundland J. Struct. Geol. 18 (1996) 975–990.
[17] W. Harland, Tectonic transpression in Caledonian Spitzbergen, Geol. Mag. 108 (1971) 27–42.
[18] B. Hobbs, W. Means, P. Williams, An outline of Structural Geology, John Wiley & Sons, 1976 571 pp.
[19] P. Hudleston, L. Lan, Information from fold shapes, J. Struct. Geol. 15 (1993) 253–264.
[20] A. James, A. Watkinson, Initiation of folding and boudinage in wrench shear and transpression, J. Struct. Geol. 16 (1994) 883–893.
[21] R. Jones, P. Tanner, Strain partitioning in transpression zones, J. Struct. Geol. 17 (1995) 793–802.
[22] R. Lacassin, J. Van Den Driessche, Finite strain determination of gneiss: application of Fry's method to porphiroid in the Southern Massif Central (France), J. Struct. Geol. 5 (1983) 245–253.
[23] J. Lee, J. Angelier, H. Chu, S. Yu, J. Hu, Plate-boundary strain partitioning along the sinistral collision suture of the Philippine and Eurasian plates: analysis of geodetic data and geological observation in southeastern Taiwan, Tectonics 17 (1998) 859–871.
[24] S. Machado, C. Garcia, R. Dias, C. Coke, A. Ribeiro, Finite strain analysis in a fold due to transpressive regime (Centro-Iberian autochthon). Comun. "XII Reunião de Geologia do Oeste Peninsular", Évora, Portugal, 1993, pp. 99–112.
[25] P. Matte, A. Ribeiro, Forme et orientation de l'éllipsoid de déformation dans la virgation hercynienne de Galice, Relations avec le plissement et hypotèses sur la génese de l'arc ibéro-armoricain 280 (1975) 2825–2828 C. R. Ac. Sc. Paris, Sér. D.
[26] A. McLeish, Strain analysis of deformed pipe rock in the Moine Thrust Zone, northwest Scotland, Tectonophysics 12 (1971) 469–503.
[27] R. Moore, Treatise of Invertebrate Paleontology. Part W, Miscellania. Supplement 1: Trace Fossils and Problematica, Geological Soceity of America, New York, 1975.
[28] V. Mount, J. Suppe, State of stress near the San Andreas fault: implications for wrench tectonics, Geology 15 (1987) 1143–1146.
[29] C. Onasch, Ability of the Fry method to characterize pressure-solution deformation, Tectonophysics 122 (1986) 187–193.
[30] R. Paulis, A new method of strain measurement using initially orthogonal planar and linear markers, Tectonophysics 34 (1976) T29–T36.
[31] C. Powell, Timing of slaty cleavage during folding of Precambrian rocks, northwest Tasmania, Geol. Soc. Am. Bull. 85 (1974) 1043–1060.
[32] J. Ramsay, Folding and Fracturing of Rocks, McGraw-Hill, New York, 1967 568 pp.
[33] J. Ramsay, M. Huber, The Techniques of Modern Structural Geology, Strain Analysis, I, Academic Press Inc., London, 1983 307 pp.
[34] J. Ramsay, D. Wood, The geometric effects of volume change during deformation processes, Tectonophysics 16 (1973) 263–277.
[35] J. Rebelo, M. Romano, A contribution to the lithostratigraphy and palaeontology of the lower Paleozoic rocks of the Moncorvo region, northeast Portugal, Comun. Serv. Geol. Portugal 72 (1986) 45–57.
[36] A. Ribeiro, Contribution à l'étude tectonique de Trás-os-Montes oriental, Mem. Serv. Geol. Portugal N.S. 24 (1974) 168.
[37] A. Ribeiro, E. Pereira, R. Dias, Structure of the Northwest of the Iberian Peninsula, in: D. Dallmeyer, E. Martinez Garcia (Eds.), Pre-Mesozoic Geology of Iberia, Springer-Verlag, 1990, pp. 220–236.
[38] A. Ribeiro, R. Dias, J. Brandão Silva, Genesis of the Ibero-Armorican Arc, Geodinamica Acta 8 (2) (1995) 173–184.
[39] P. Richard, P. Cobbold, Experimental insights into partitioning of fault motions in continental convergent wrench zones, Annales Tectonicae 2 (1990) 35–44 Special IV.
[40] D. Sanderson, Structural variation across the northern margin of the Variscides in NW Europe, in: D. Hutton, D. Sanderson (Eds.), Variscan Tectonics of the North Atlantic Region, Geol. Soc., 6, 1984, pp. 449–458.
[41] D. Sanderson, W. Marchini, Transpression, J. Struct. Geol. 6 (5) (1984) 449–458.
[42] C. Teyssier, B. Tikoff, Strike–slip partitioned transpression of the San Andreas fault system: a lithospheric approach, in: R. Holdsworth, R. Strachan, J. Dewey (Eds.), Continental Transpression and Transtension Tectonics, Geol. Soc., 135, 1998, pp. 143–158.
[43] C. Teyssier, B. Tikoff, M. Markley, Oblique plate motion and continental tectonics, Geology 23 (5) (1995) 447–450.
[44] B. Tikoff, C. Teyssier, Strain modeling of displacement-field partitioning in transpressional orogens, J. Struct. Geol. 16 (11) (1994) 1575–1588.
[45] B. Tikoff, K. Peterson, Physical models of transpressional folding, J. Struct. Geol. 20 (1998) 1497–1512.
[46] J. Treagus, S. Treagus, Transected folds and transpression: how are they related, J. Struct. Geol. 14 (1992) 361–367.
[47] R. Twiss, E. Moores, Structural Geology, W.H. Freeman and Company, 1992 532 pp.